Supplementary Information for

Rapid and sensitive detection of formaldehyde using portable 2-dimensional gas chromatography equipped with photoionization detectors

Hongbo Zhu,[ab] Jinyan She,[ab] Menglian Zhou,[ab] and Xudong Fan*[ab]

[a]Department of Biomedical Engineering, University of Michigan, 1101 Beal Avenue, Ann Arbor, Michigan 48109, United States

[b]Center for Wireless Integrated MicroSensing and Systems (WIMS^2), University of Michigan, Ann Arbor, MI, 48109, United States

*Email address: xsfan@umich.edu

Table S1. Regulated formaldehyde exposure limits.

Institution	**Regulated exposure limit ppb (V/V)**	**Remarks**
National Institute for Occupational Safety and Health (USA)	16[I]	Time-weighted average (TWA) concentrations for up to a 10-hour workday during a 40-hour workweek
	100[II]	No more than 15 minutes exposure at any time during a day
Occupational Safety and Health Administration (USA)	750[III]	Eight-hour TWA, which is an average value of exposure over an eight-hour work shift.
	2000[II]	Average value over 15 minutes of exposure
American Conference of Governmental Industrial Hygienists	300[IV]	Recommended ceiling limit, not to be exceeded at any time during a day
World Health Organization	81	Maximum level in non-occupational settings
California Air Resources Board	2[V]	

I, Recommended exposure limit

II, Ceiling limit, should not be exceeded

III, Permissible exposure limits, maximum concentrations of chemicals to which a worker may be exposed

IV, Threshold limit values, guidelines for the level of exposure that the typical worker can be exposed without adverse health effects.

V, Chronic reference exposure limit

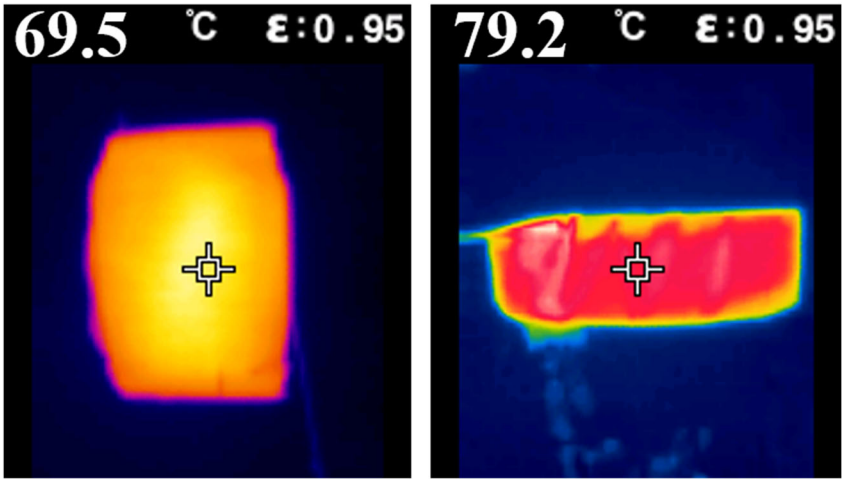

Figure S1. Infrared thermal image of the (A) heated 1st–dimensional column and (B) the heated 2nd–dimensional column taken with a FLIR TG165 infrared camera. The excessive temperature difference on the column coil edge was proved to be pseudomorphism by multi-point inspection with a thermocouple, which might be caused by infrared reflection from wrinkles on the column coil surface.

μHDBD-PID design and fabrication

In this design, a sandwich structure (glass/silicon/glass) was employed to build the helium plasma chamber, the fluidic channel, and the ionization channel. The fabrication process is described in Figure S2. A 380-μm thick silicon was anodically bonded to 100-μm thick glass (Figure S2A). Then, deep reactive-ion etching was used to etch through the silicon wafer and create the features shown in Figure S2B. Finally, a 100-nm thick platinum electrode used for high-voltage barrier discharge induction was deposited on the outer surface of the glass wafer on each side after glass/silicon and glass anodic bonding. The engineering drawing of the μHDBD-PID is shown in Figure S2E. Since the gas flow insulation design included quadri-venting ports and a shielding wall, the plasma chamber was better isolated from the analyte inlet channel (shown in Figure S3B). Thus, the auxiliary helium flow was not required to be set at a high level to avoid the contamination by the flow from ionization channel. A flow resistor (see Figure 3C) was applied to control the auxiliary flow at a rate of 5 mL/min in all tests. In addition, the shielding wall helped reduce the baseline signal and prevent signal overload caused by electric arcs in the plasma chamber.

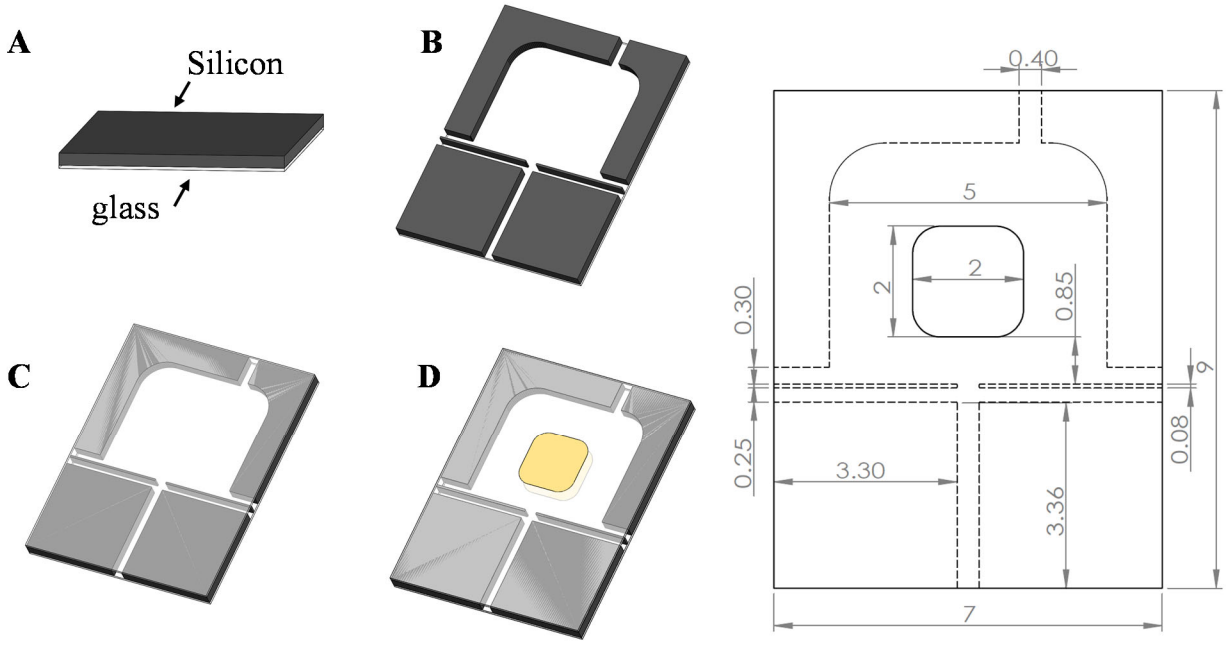

Figure S2. μHDBD-PID fabrication procedure (A) Anodically bonded glass and silicon. (B) Features of plasma chamber, fluidic channel, and ionization channel created by deep reactive-ion etching. (C) Another layer of glass anodically bonded to silicon. (D) Illustration of μHDBD-PID after high-voltage barrier discharge electrode deposition. (E) Engineering drawing of the μHDBD-PID in the units of mm.

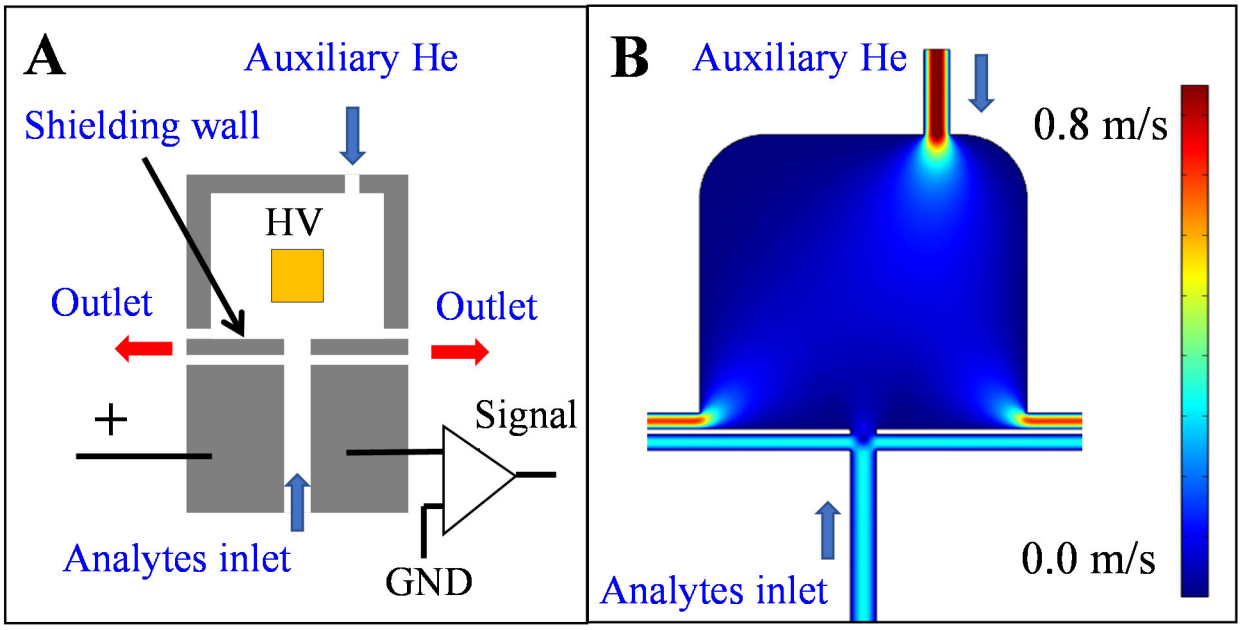

Figure S3. (A) Electric and fluidic connection of the μHDBD-PID (B) Fluidic simulation result by COMSOL Multiphysics® with a flow rate of 2 mL/min and 5 mL/min at the analytes inlet and the auxiliary He inlet, respectively.

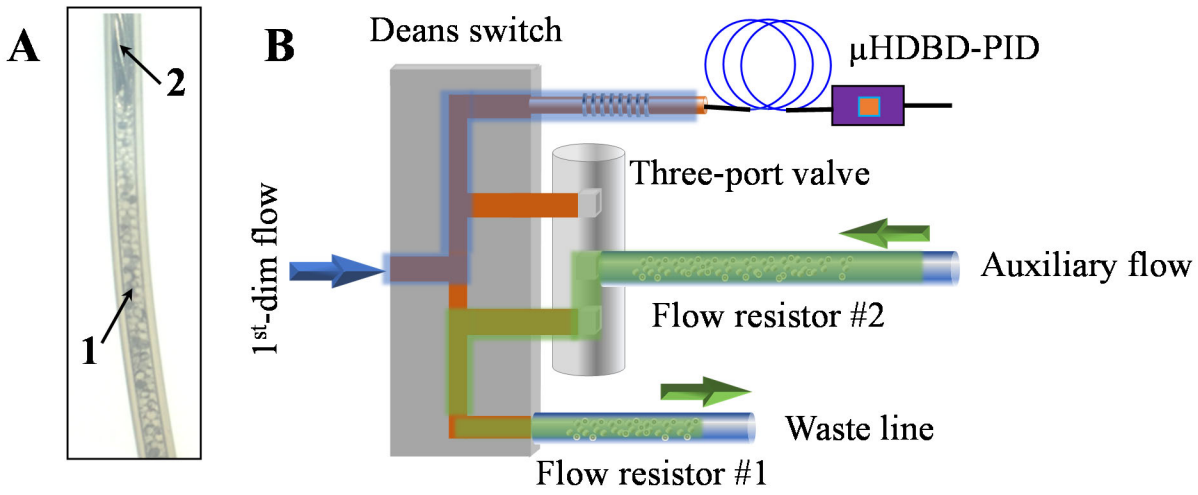

Figure S4. (A) Picture of a flow resistor made from polytetrafluoroethylene tube (1/32 inch o.d., 0.48 mm i.d.) filled with glass beads (1) and sealed by a metal wire (2). (B) Illustration of the fluidic arrangement for the micro-Deans switch. The flow resistor #1 provided the same flow resistance as the 2nd–dimensional fluidic resistance (including the thermal injector, 2nd–dimensional column, and μHDBD-PID) and was installed in the waste line for flow balance. The flow resistor #2 provided the same flow resistance as the 1st–dimensional fluidic resistance and was installed at the upstream of the three-port valve that controlled the auxiliary flow of the micro-Deans switch.

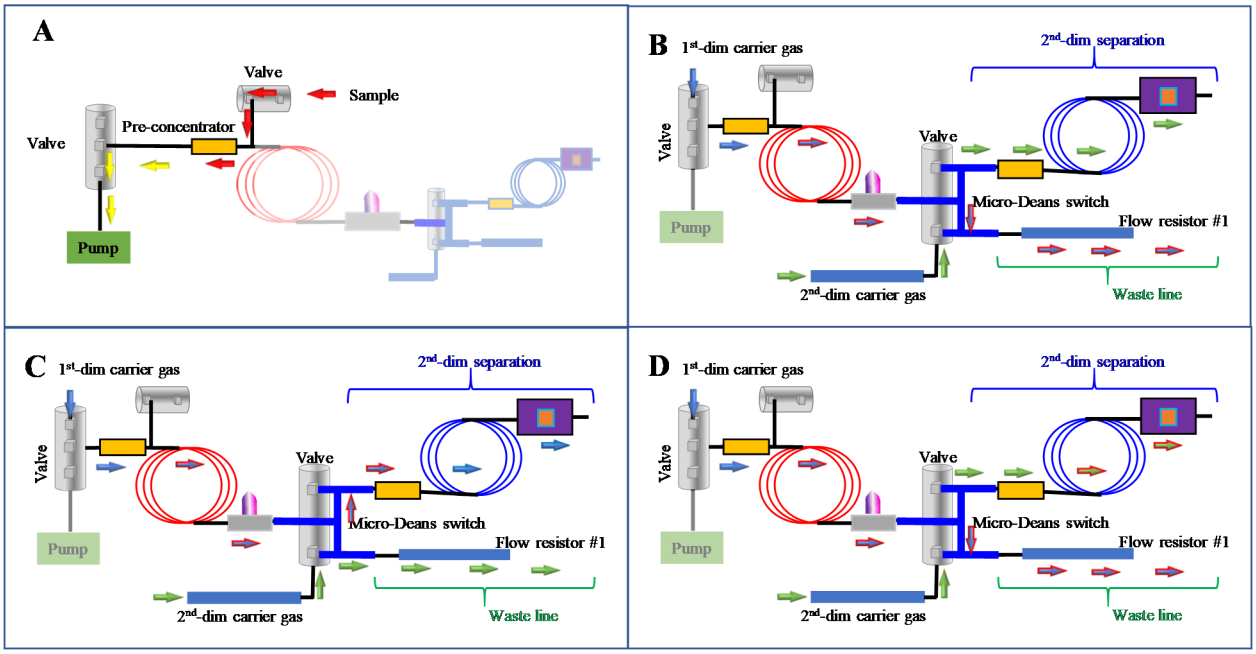

Figure S5 Gas flow layouts at (A) sampling, (B) 1-D separation, (C) target cutting, and (D) 1st- and 2nd-dimensional separation.

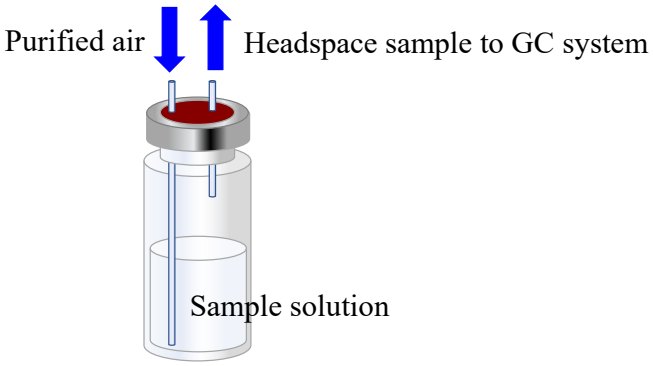

Figure S6. Illustration of VOCs vapor generation setup that consisted of a 20-mL vial filled with 10 mL sample solution with an inlet and an outlet for purging purified air and GC sampling, respectively.

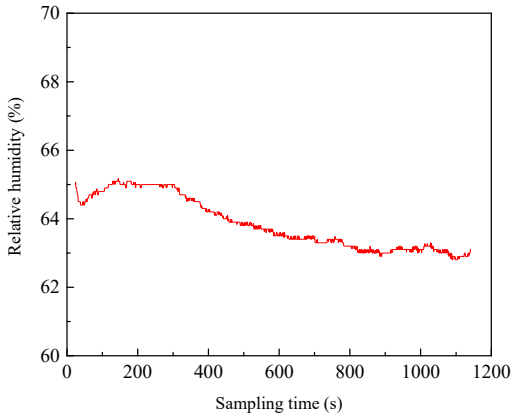

Figure S7. Relative humidity level measured by a dew-point sensor at the outlet of the sample purge setup at 23 ℃.